

# UC Irvine

## UC Irvine Previously Published Works

### Title

Multimodal Imaging in Ocular Siderosis

### Permalink

<https://escholarship.org/uc/item/83g4j26t>

### Journal

Journal of VitreoRetinal Diseases, 5(1)

### ISSN

2474-1264

### Authors

Bui, Anh D  
Diep, Anna L  
Lin, Qiyin  
et al.

### Publication Date


2021

### DOI

10.1177/2474126420962020

Peer reviewed

# Multimodal Imaging in Ocular Siderosis

Anh D. Bui, MD, PhD<sup>1,2</sup>, Anna L. Diep, BS<sup>2</sup> , Qiyin Lin, PhD<sup>3</sup>, Donald S. Minckler, MD<sup>4</sup>, Andrew W. Browne, MD, PhD<sup>4,5,6</sup>, and Angeline L. Wang, MD<sup>4,7</sup>

Journal of VitreoRetinal Diseases  
2021, Vol. 5(1) 81-86  
© The Author(s) 2020  
Article reuse guidelines:  
sagepub.com/journals-permissions  
DOI: 10.1177/2474126420962020  
jvrd.sagepub.com



## Abstract

**Purpose:** This report aims to characterize ocular changes in a case of ocular siderosis with iron toxicity using multimodal imaging and electroretinography. **Methods:** A 34-year-old woman presented with ocular siderosis of the left eye following penetrating injury with an iron-containing foreign body. The patient's uncorrected visual acuities were 20/60 and 20/150 in the right and left eye, respectively, with abnormal pupillary function and presence of a cataract in the left eye. She underwent successful intraocular foreign body removal and cataract surgery with no postoperative complications. Cone contrast threshold (CCT), full-field electroretinogram, spectral-domain optical coherence tomography (OCT), and OCT angiography (OCTA) were used to characterize ocular alterations preoperatively and postoperatively. **Results:** CCT color vision testing showed abnormal color vision, and OCTA revealed increased vascular flow density associated with the foreign body. **Conclusions:** CCT color vision testing, OCTA, OCT, and full-field electroretinogram can characterize retinal changes in cases of ocular siderosis.

## Keywords

ocular siderosis, iron toxicity, optical coherence tomography, OCT angiography, full-field electroretinogram, intraocular foreign body

## Introduction

Ocular siderosis is a degenerative process caused by retention of an iron-containing intraocular foreign body (IOFB). Clinical symptoms may take weeks to years to manifest and can include decreased visual acuity (VA), conjunctival hyperemia, iris heterochromia, secondary glaucoma, and lens opacity.<sup>1</sup> Once ocular siderosis is identified, timely removal of the IOFB must be performed to prevent irreversible changes and retinal damage secondary to iron-related toxicities. We document a case of ocular siderosis with the use of cone contrast threshold (CCT) color vision testing, optical coherence tomography (OCT), OCT angiography (OCTA), and full-field electroretinogram (ffERG).

## Methods

### Case Report

A 34-year-old woman presented with a history of penetration by a metallic foreign body in her left eye while hammering a nail 8 months prior. The patient reported to an outside hospital 1 day after the initial incident, where the IOFB was partially extracted at the slitlamp microscope. The patient was discharged with ciprofloxacin eye drops for 7 days and an ophthalmology referral. However, her left eye's VA continued to progressively worsen. She did not report subjective changes in color vision. She denied any previous notable ocular history.

On presentation to our institution, her VA was 20/60 (pinhole 20/30) in the right eye and 20/150 (pinhole 20/50) in the left eye. The right pupil constricted with illumination from 5.5 mm to 3 mm. The left pupil was dilated and fixed at 7 mm (Figure 1A). Application of 0.1% pilocarpine caused right and left pupil constriction to 3 mm and 4 mm, respectively (Figure 1B). Slitlamp examination demonstrated a metallic foreign body embedded in the temporal sclera (Figure 1, C and D). Diffuse pigmentary changes of the anterior lens capsule (Figure 1E) and a cataract in the left eye were observed. Results of a posterior segment examination and fundus autofluorescence

<sup>1</sup> Department of Ophthalmology, University of California, San Francisco, San Francisco, CA, USA

<sup>2</sup> School of Medicine, University of California, Irvine, Irvine, CA, USA

<sup>3</sup> Irvine Materials Research Institute, University of California, Irvine, Irvine, CA, USA

<sup>4</sup> Gavin Herbert Eye Institute, University of California, Irvine, Irvine, CA, USA

<sup>5</sup> Department of Biomedical Engineering, University of California, Irvine, Irvine, CA, USA

<sup>6</sup> Institute for Clinical and Translational Science, University of California, Irvine, Irvine, CA, USA

<sup>7</sup> Department of Ophthalmology, UT Southwestern Medical Center, Dallas, TX, USA

### Corresponding Author:

Anh D. Bui, MD, PhD, Department of Ophthalmology, University of California, San Francisco, 10 Koret Way, San Francisco, CA 94143, USA.

Email: anh.bui@ucsf.edu

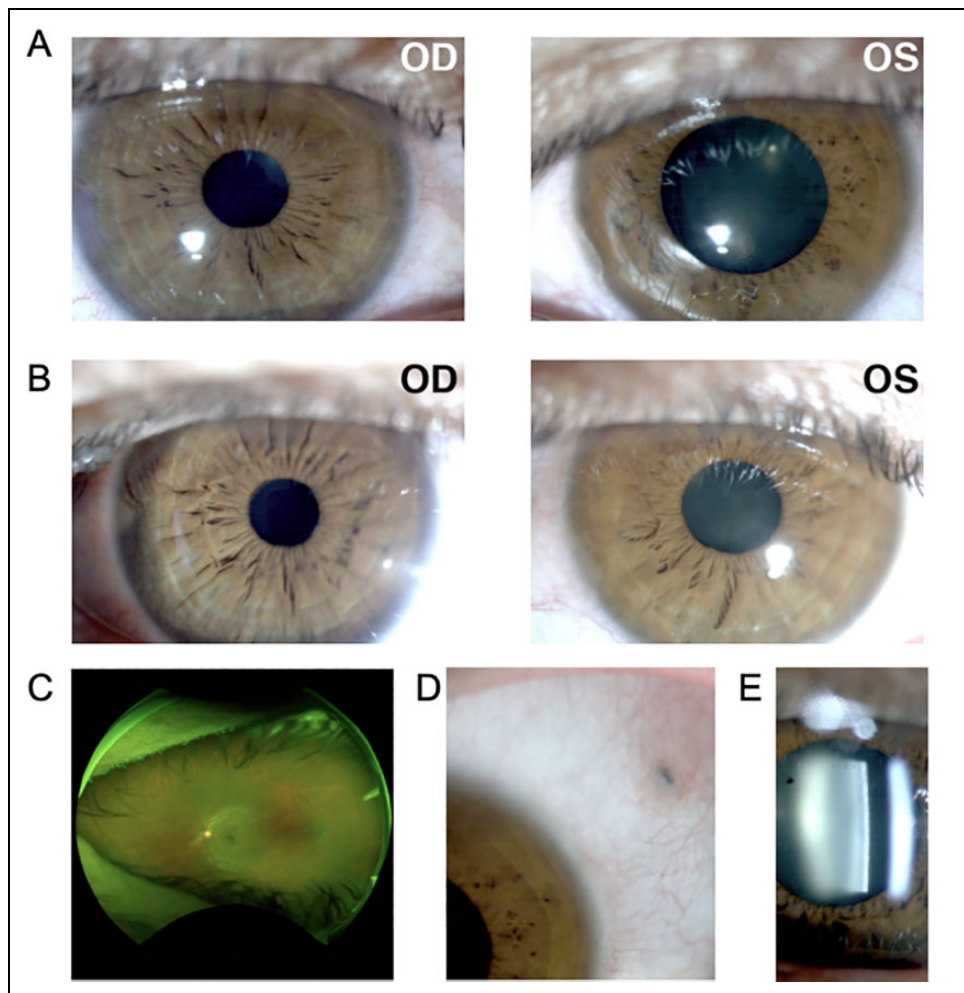


**Figure 1.** Intraocular foreign body and pupillary changes. (A) Prepilocarpine and (B) postpilocarpine test in the right (OD) and left (OS) eyes. (C) Color fundus photograph and (D) external photograph of the left eye, showing the intraocular foreign body located in the superotemporal pars plana. (E) Slitlamp photograph showing mottling and pigmentation of the left anterior lens capsule.

and color fundus photographs were unremarkable. The metallic body was visible on scleral depressed examination.

OCTA (Zeiss Cirrus 5000) of both the superficial and deep capillary plexuses revealed a 38% greater parafoveal vascular flow density in the left eye compared with the right eye (Figure 2A), calculated using ImageJ software with the parafoveal region defined as an annulus with an outer diameter of 1.25 mm and an inner diameter of 0.3 mm centered at the fovea.<sup>2</sup> Spectral-domain OCT (SD-OCT; Heidelberg Spectralis) showed subtle macular thickening in the left eye compared with the right eye (Figure 2B). Full-field ERG showed reduced amplitudes in the left eye on all stimuli, with greatest changes noted on dark adaptation (Figure 2C). En face ellipsoid zone analysis was unremarkable (Figure 2D).

## Results

To remove the IOFB, an angled 20-gauge microvitrectoretinal blade was used to incise the sclera's full thickness superiorly

and inferiorly to the metallic foreign body. The 0.4-mm long metallic foreign body was removed with a magnet and forceps, and a limited vitrectomy was performed around the site of the scleral incision. Postoperative recovery was uneventful. ColorDx CCT HD (Konan Medical) color vision testing results 1 month following IOFB removal were normal in the right eye but showed significantly decreased green and blue color discrimination in the left eye (Figure 3A).

Seven weeks following IOFB removal, the patient underwent cataract extraction and intraocular lens placement. Histological analysis with Prussian blue staining of the anterior lens capsule showed widespread deposition of iron in the lens' epithelial cells (Figure 4A). Scanning electron microscopy and energy dispersive x-ray spectroscopy analysis confirmed that the foreign body was composed of iron oxide with trace manganese, phosphorus, and silicon (Figure 4, B and C). VA in the patient's left eye post cataract surgery was 20/20 and has remained stable for 2 years. Pupillary reactivity also significantly improved in the left eye, with constriction on illumination from 4.5 mm to 3 mm.

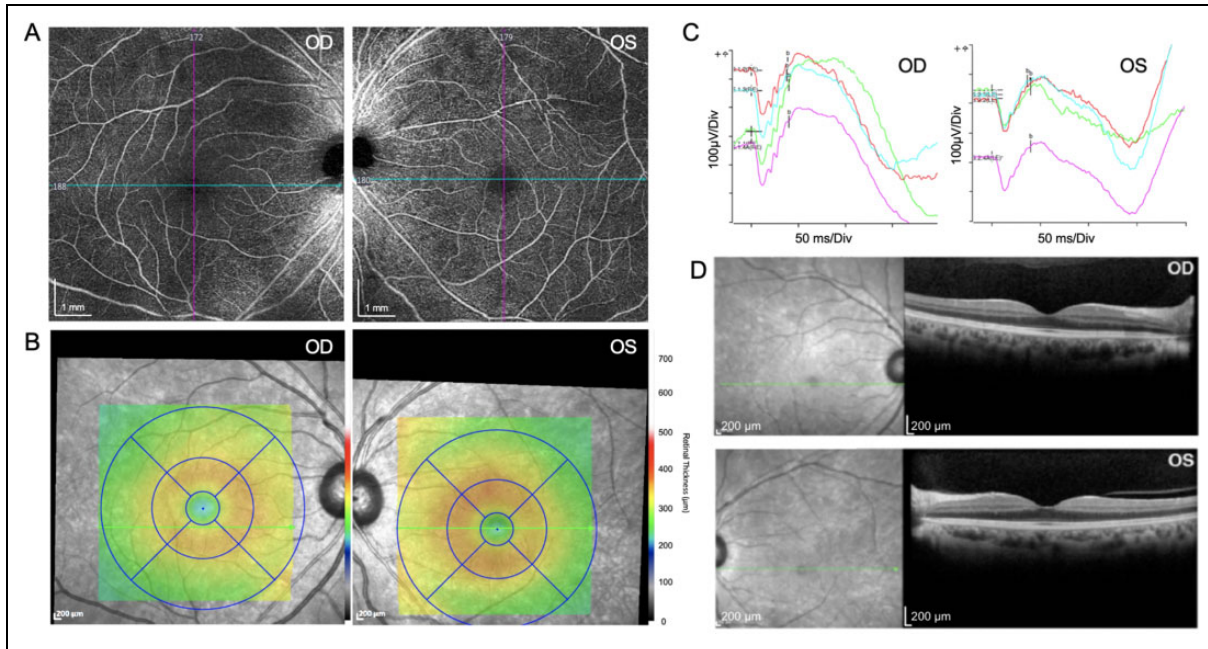


**Figure 2.** Iron-induced retinotoxicity on full-field electroretinogram and optical coherence tomography (OCT) imaging. (A) OCT angiography demonstrating a 38% increased parafoveal vascular flow density in the left eye compared with the right eye. (B) Spectral-domain OCT imaging revealing mild macular thickening in the left eye. (C) Full-field electroretinogram showing a reduction of the b-wave amplitude in the left eye compared with the right eye. (D) Spectral-domain OCT cross-sectional images were unremarkable. OD indicates right eye; OS, left eye.

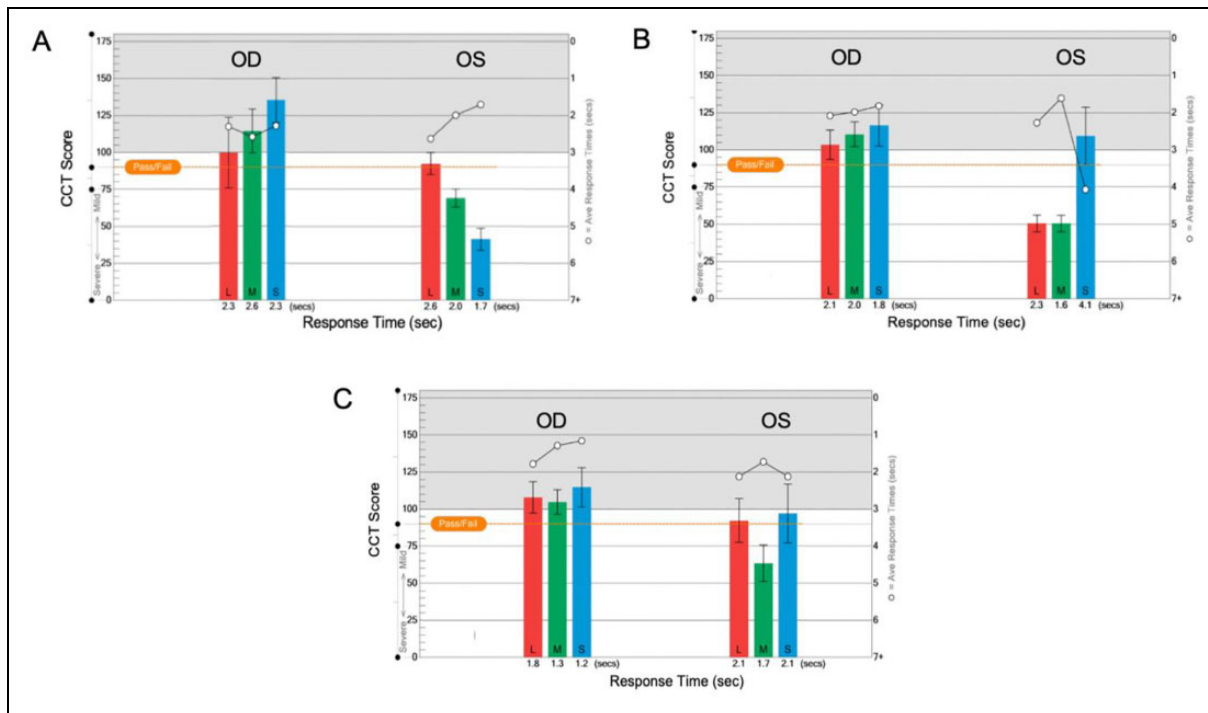


**Figure 3.** ColorDx Cone contrast threshold (CCT) HD color vision testing. (A) CCT testing 1 month after intraocular foreign body (IOFB) removal showing markedly reduced green and blue discrimination in the left eye compared with the right eye. (B) CCT testing 3 months after IOFB removal and 1.5 months after cataract extraction showing normal blue discrimination but reduced red and green discrimination in the left eye. (C) CCT testing 17 months after IOFB removal and 15.5 months after cataract extraction showing normalized red and blue discrimination but persistently decreased green discrimination in the left eye. L indicates retinal L-cone; M, retinal M-cone; OD, right eye; OS, left eye; S, retinal S-cone.

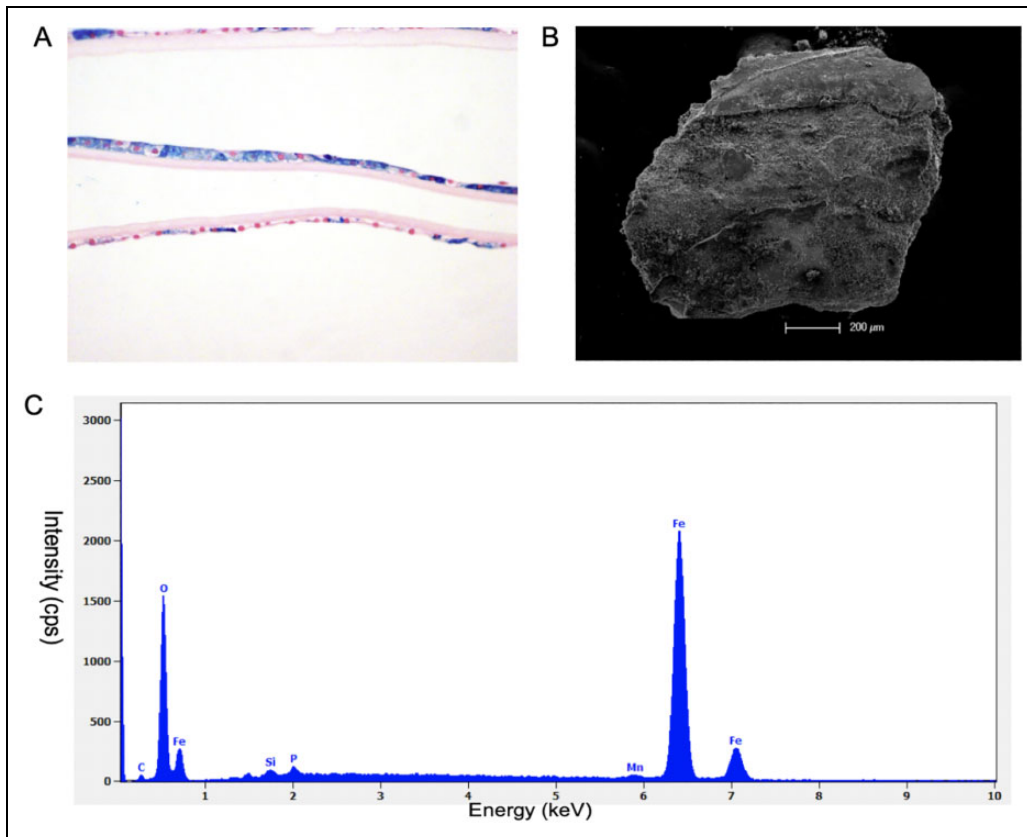


**Figure 4.** Analysis of iron intraocular foreign body. (A) Histological examination with Prussian blue staining demonstrating widespread deposition of iron in the lens' epithelial cells of the anterior capsule. (B) Scanning electron microscopy of the metallic foreign body. (C) Energy x-ray spectroscopy analysis confirming the presence of iron along with trace amounts of manganese, silicon, and phosphorus.

CCT color vision testing 3 months following IOFB removal and 1.5 months following cataract extraction showed normal blue color discrimination but deficient red and green color discrimination in the left eye (Figure 3B). CCT testing performed again 17 months after IOFB removal showed normal red and blue color discrimination but decreased green color discrimination in the patient's left eye (Figure 3C). Another OCTA of both superficial and deep capillary plexuses performed 3 months following IOFB removal demonstrated a 9% greater parafoveal vascular flow density in the left eye compared with the right eye, normalized compared with 38% preoperatively (Figure 5A). A second SD-OCT imaging 17 months after IOFB removal showed comparable macular thickness between the right and left eyes (Figure 5B). Further ffERG testing performed 6 months following IOFB removal also revealed normalization of the b-wave amplitude in the left eye (Figure 5C).

## Conclusions

Iron plays an essential role in the photoreceptor cell signal transduction cascade in the retina.<sup>3</sup> However, iron is toxic at high levels and can lead to the formation of free radicals,

oxidative damage, and cell death.<sup>3</sup> In the retina, iron toxicity can precipitate events such as retinal detachment, pigment epithelial atrophy, and arteriole stenosis.<sup>1</sup> Iron metabolism disorders such as Friedreich ataxia and hemochromatosis have also been associated with retinal degeneration.<sup>4</sup>

This patient had classic clinical manifestations of iron toxicity, including paralytic mydriasis and parasympathetic neuropathy of the pupil, as well as cataract formation and iron deposition beneath the anterior lens capsule, consistent with previous case reports.<sup>5,6</sup> ERG has been established as the primary modality to measure retinal changes in patients with IOFB.<sup>7</sup> Loss of function of the photoreceptors due to iron toxicity has been well described with deterioration of b-wave ERG amplitudes, which was observed in this patient.<sup>5</sup>

CCT color testing in this patient presented a unique opportunity to measure the subtle changes in color vision following IOFB extraction. CCT color testing selectively stimulates retinal L-cones (red), M-cones (green), and S-cones (blue). It is performed with a series of tumbling Landolt-C optotypes presented in randomized directions with varying contrast levels to the patient. The patient is required to indicate the orientation of the gap in the "C" stimulus (forced-choice letter-recognition

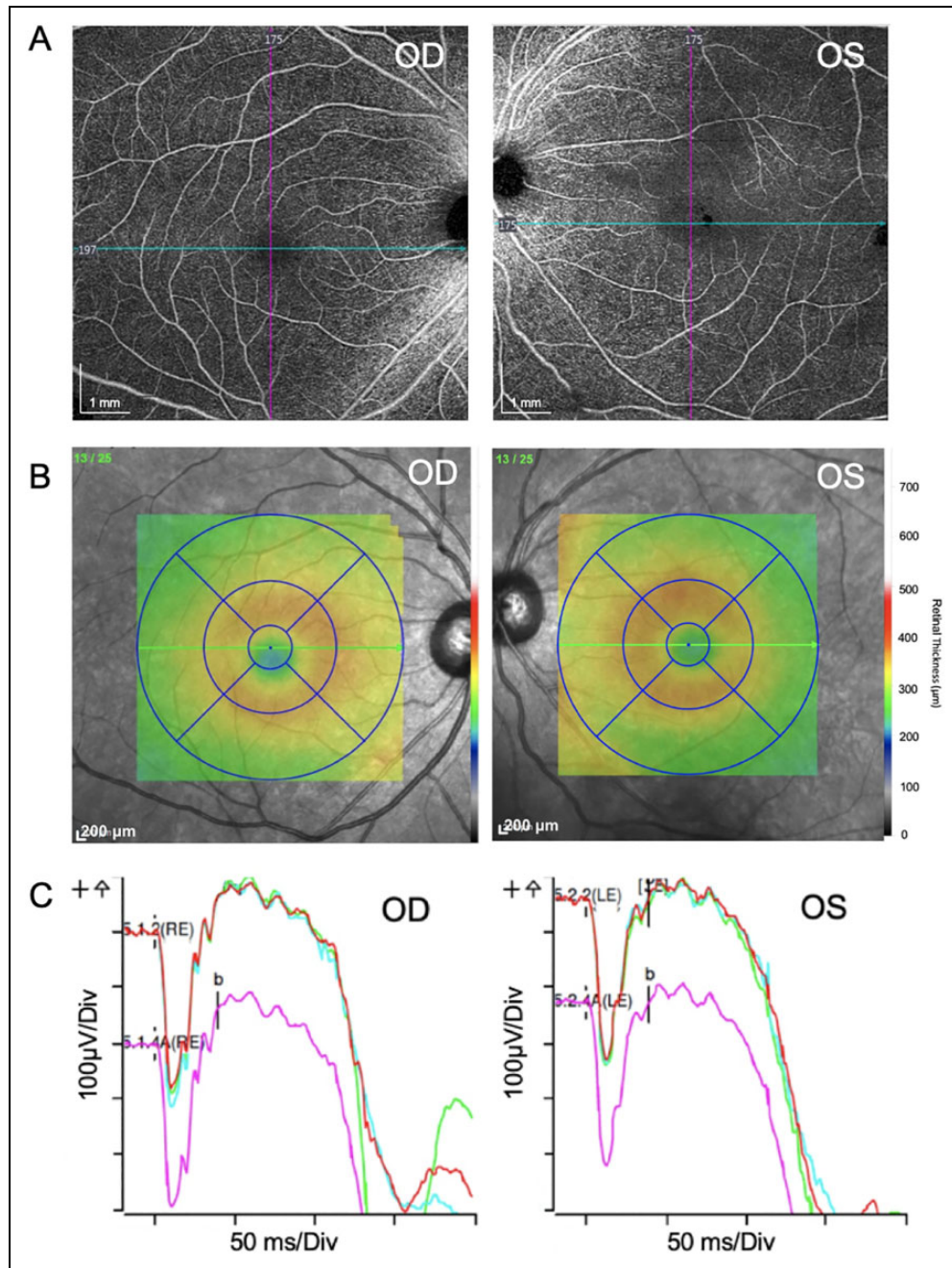


**Figure 5.** Postsurgical imaging on full-field electroretinogram (ERG) and optical coherence tomography (OCT). (A) OCT angiography demonstrating comparable parafoveal vascular flow density in the left eye compared with the right eye. (B) Spectral-domain OCT imaging revealing comparable macular thickness between the left eye and right eye. (C) Full-field ERG showing normal b-wave amplitude in the left eye, which had improved compared with prior to removal of the intraocular foreign body. LE indicates left eye; OD, right eye; OS, left eye; RE, right eye; 50ms/Div, 50 milliseconds per division.

task). The contrast of the stimuli is continuously refined to determine the final contrast threshold, minimizing the standard error.

Color vision has been shown to be reduced in patients with cataracts.<sup>8,9</sup> However, in this patient's case, only blue color vision returned to normal following cataract surgery. Red and green color discrimination was significantly impaired 1.5

months following cataract extraction, and green color discrimination remained significantly impaired for more than 1 year post cataract surgery. Permanent changes in color vision are most likely the consequence of cytotoxicity to the neurosensory retina.<sup>1</sup> A greater density of L- and M-cones (red and green cones) exist in the fovea,<sup>10</sup> but it is unclear why a greater effect was seen on the green cones.

In the case reported here, the patient's OCTA prior to IOFB removal showed increased vascular flow density in the left eye with the IOFB compared with the right eye. Increased vascular flow density could be due to increased vascularization or congestion. One should note that OCTA has known limitations, including projection and motion artifacts, that preclude a detailed understanding of the spatial vasculature characteristics. However, we do not believe our observations by OCTA are artifactual because we also observed increased retinal thickness on SD-OCT. These 2 independent measurements were consistent with an increase in vascular flow density. Both OCTA and SD-OCT findings also became comparable between the right eye and left eye after IOFB removal. We expect that continued improvements in OCT will permit further analysis of these sequelae.

This case highlights the importance of a complete characterization of ocular siderosis through multiple imaging modalities. Although ERG has been well established as a criterion standard for cases of IOFB, CCT color testing combined with OCTA may be surrogate functional assays for detecting siderosis and monitoring changes following surgical intervention.

#### Authors' Note

All authors attest that they meet the current International Committee of Medical Journal Editors criteria for authorship.

#### Ethical Approval

This case report was conducted in accordance with the Declaration of Helsinki. The collection and evaluation of protected patient health information was performed in a Health Insurance Portability and Accountability Act (HIPAA)-compliant manner.

#### Statement of Informed Consent

Written informed consent was obtained from the patient for publication of this case report and the accompanying images.

#### Declaration of Conflicting Interests


The author(s) declared no potential conflicts of interest with respect to the research, authorship, and/or publication of this article.

#### Funding

The author(s) disclosed receipt of the following financial support for the research, authorship, and/or publication of this article: This work was supported by an unrestricted grant from Research to Prevent

Blindness and a National Institutes of Health KL2 grant from the Institute for Clinical and Translational Science (grant no. KL2 TR001416).

#### ORCID iD

Anna L. Diep, BS  <https://orcid.org/0000-0002-2711-6885>

#### References

1. Xie H, Chen S. Ocular siderosis. *Eye Sci.* 2013;28(2):108-112.
2. Hwang TS, Gao SS, Liu L, et al. Automated quantification of capillary nonperfusion using optical coherence tomography angiography in diabetic retinopathy. *JAMA Ophthalmol.* 2016;134(4):367-373. doi:10.1001/jamaophthalmol.2015.5658
3. Song D, Dunaief JL. Retinal iron homeostasis in health and disease. *Front Aging Neurosci.* 2013;5:24. doi:10.3389/fnagi.2013.00024
4. Alldredge CD, Schlieve CR, Miller NR, Levin LA. Pathophysiology of the optic neuropathy associated with Friedreich ataxia. *Arch Ophthalmol.* 2003;121(11):1582-1585. doi:10.1001/archophth.121.11.1582
5. Hope-Ross M, Mahon GJ, Johnston PB. Ocular siderosis. *Eye (Lond).* 1993;7(Pt 3):419-425. doi:10.1038/eye.1993.83
6. Sneed SR, Weingeist TA. Management of siderosis bulbi due to a retained iron-containing intraocular foreign body. *Ophthalmology.* 1990;97(3):375-379. doi:10.1016/s0161-6420(90)32578-2
7. Sahay P, Kumawat D, Gupta S, et al. Detection and monitoring of subclinical ocular siderosis using multifocal electroretinogram. *Eye (Lond).* 2019;33(10):1547-1555. doi:10.1038/s41433-019-0442-y
8. Ao M, Li X, Qiu W, Hou Z, Su J, Wang W. The impact of age-related cataracts on colour perception, postoperative recovery and related spectra derived from test of hue perception. *BMC Ophthalmol.* 2019;19(1):56. doi:10.1186/s12886-019-1057-6
9. Mehta U, Diep A, Nguyen K, et al. Quantifying color vision changes associated with cataracts using cone contrast thresholds. bioRxiv. Preprint posted online June 28, 2020. doi:10.1101/2020.06.27.175570
10. Curcio CA, Hendrickson AE. Organization and development of the primate photoreceptor mosaic. In: Osborne N, Chader J, eds. *Progress in Retinal Research.* Pergamon Press; 1991:89-120. doi:10.1016/0278-4327(91)90010-Y